Article

Classification of Peruvian Flours via NIR Spectroscopy Combined with Chemometrics

Milton Martínez-Julca [1,*], Renny Nazario-Naveda [2] , Moises Gallozzo-Cárdenas [3], Segundo Rojas-Flores [4] , Hector Chinchay-Espino [5], Amilu Alvarez-Escobedo [5] and Emzon Murga-Torres [6]

1   Departamento de Ciencias Virtual Campus, Universidad Privada del Norte, Trujillo 13007, Peru
2   Vicerrectorado de Investigación, Universidad Autónoma del Perú, Lima 15842, Peru; scored731@gmail.com
3   Facultad de Ciencias de la Salud, Universidad César Vallejo, Trujillo 13001, Peru; mmgallozzo@ucvvirtual.edu.pe
4   Instituto de Investigación en Ciencia y Tecnología de la Universidad César Vallejo, Trujillo 13001, Peru; segundo.rojas.89@gmail.com
5   Departamento de Ciencias, Universidad Privada del Norte, Chorrillos 15054, Peru; hector.chinchay@upn.edu.pe (H.C.-E.); amilu.alvarez@upn.edu.pe (A.A.-E.)
6   Laboratorio de Investigación Multidisciplinario, Universidad Privada Antenor Orrego, Trujillo 13008, Peru; ee_mt_66@hotmail.com
*   Correspondence: mmartinezjulca@gmail.com

Abstract: Nowadays, nutritional foods have a great impact on healthy diets. In particular, maca, oatmeal, broad bean, soybean, and algarrobo are widely used in different ways in the daily diets of many people due to their nutritional components. However, many of these foods share certain physical similarities with others of lower quality, making it difficult to identify them with certainty. Few studies have been conducted to find any differences using practical techniques with minimal preparation and in short durations. In this work, Principal Component Analysis (PCA) and Near Infrared Spectroscopy (NIR) were used to classify and distinguish samples based on their chemical properties. The spectral data were pretreated to further highlight the differences among the samples determined via PCA. The results indicate that the raw spectral data of all the samples had similar patterns, and their respective PCA analysis results could not be used to differentiate them. However, pretreated data differentiated the foods in separate clusters according to score plots. The main difference was a C-O band that corresponded to a vibration mode at 4644 cm^{-1} associated with protein content. PCA combined with spectral analysis can be used to differentiate and classify foods using small samples through the chemical properties on their surfaces. This study contributes new knowledge toward the more precise identification of foods, even if they are combined.

Keywords: PCA; NIR spectroscopy; Peruvian flours; chemometrics; maca

1. Introduction

Grains such as maca (*Lepidium meyenii*), algarrobo (*Prosopis pallida*), soybean (*Glycine max* L.), oatmeal, and broad bean (*Vicia faba*) are used as popular dietary supplements in Peru [1,2]. Maca has been demonstrated to exhibit medical benefits, such as antifatigue, anti-osteoporosis, spermatogenetic, and energy-increasing properties; algarrobo contains high amounts of dietary fiber and protein; soybean has been researched due to its positive benefits, such as its ability to improve bone mass, ameliorate the effects of menopause, and reduce cholesterol; oatmeal is a basic ingredient in many dietary supplements due to its amino acid and fiber content; and clinical studies have demonstrated that broad beans offer benefits in Parkinson's disease due to levels of L-dopa, addressing a key factor of neurological health [3–7]. Currently, these products have a high demand in terms of consumption due to their high energy content and the health benefits they offer; likewise, these foods tend to have increased prices due to their positive impacts on diets [8]. These

foods are manufactured and packaged in the agri-food industry, with risks of either natural contamination or contamination due to bad practices in the production process due to the diversity of manufactured products. It is also possible to find adulterated products on the market that do not meet the minimum quality conditions or offer the promoted benefits [8–10]. The materials most used for adulteration are inexpensive compared to products based on original flour, and in the food market, this situation generates economic and health problems for consumers [11,12]. On the other hand, some flour-based products have similar physical characteristics in terms of color, texture, shape, density, and chemical properties, making them potential candidates for use as inputs in flour adulteration [9,11,13–15].

There are various techniques for the identification of foods through their chemical, physical, protein, and genetic characteristics, including mass spectrometry (MS), polymerase chain reaction (PCR) analysis, high-performance liquid chromatography (HPLC), and nuclear magnetic resonance spectroscopy (NMRS); these methods have high sensitivity but require special sample preparation for food characterization [16–21]. For example, NMRS, when applied to complex mixtures, has some disadvantages in the resulting spectrum because many signals can overlap [22]. On the other hand, near-infrared spectroscopy is a versatile technique due to its speed, lack of destructiveness, and minimal or total lack of sample preparation requirements [23,24]; however, it still presents some challenges that must be overcome in order for it to be a widely used technique. Some foods have similar NIR spectra due to their nature and chemical composition, hampering the ability to differentiate samples directly by means of this technique. One possible option for overcoming this challenge is principal component analysis (PCA) or Soft Independent Modeling of Class Analogy (SIMCA). Notably, PCA and SIMCA are unsupervised and supervised classifications, respectively. Supervised classification is used for prediction, while unsupervised classification is used for analysis and clustering (groups of samples) based on spectral properties. PCA is used to evaluate the inherent characteristics of a spectral data set as well as slight differences between spectra [25–27], while SIMCA mainly focuses on the similarities between samples within a group rather than the differences between the groups [27]. PCA mainly examines the relationships between variables (wavelength or wavenumber) and samples. It reduces the dimensions of a data set; that is, the original variables of the data set are reduced to a few new variables, which are known as principal components (PCs). The total variation of the analyzed data set is best explained by the PCs, and each principal component is independent [28]. The first principal component (PC-1) can be used to detect differences between samples because it represents the largest variation from the original data set, while the second principal component (PC-2) explains better the variation shown by the third principal component (PC-3), and so on [29]. Another classification type is partial least squares discriminant analysis (PLS-DA). This algorithm is used as a model for discriminative variable selection, restricting attention mainly to predictive modeling. Theoretically, PLS-DA is a combination of dimensionality reduction and discriminant analysis in one algorithm. Additionally, the algorithm does not necessarily fit a set of data to a particular distribution, making it more flexible than other algorithms. Because of this, this method has countless applications, including food analysis [30–32]. Lasalvia et al. (2022) used both simulated and experimental vibrational spectra to investigate the ability of PCA-LDA and PLS-DA to discriminate spectra related to different classes. The results showed that in terms of accuracy in classifying FTIR spectra, the PCA-LDA model seemed a little better than the PLS-DA model [33]. In certain cases, an NIR spectrum shows a change in the baseline and the presence of noise. Spectral preprocessing methods have been used to solve these problems—to name a few, standard normal variation (SNV), first-derivative Savitzky–Golay, and detrending methods are used to remove changes in baseline offset, baseline vertical offset, and baseline deviation in a spectral signal, respectively [34–39].

In one study, a chemometrics analysis was performed to authenticate Andean grain flours using mid-infrared spectroscopy and discriminate flour samples using protein, fatty acid, and fat profiles [40]. In another study, Raman spectroscopy in combination with PCA was used to discriminate cereal flour species; in this study, a PCA loading plot explained

that changes in starch and protein signals allowed for the discrimination of the samples [41]. Due to the similar physical characteristics of the mentioned foods, they can be easily confused, and this can be used to create adulterated products with lower quality using cheap grains [42,43]. In another study, a hyperspectral image technique and multivariate statistical process control were useful in detecting adulterations of wheat flour in the presence of different grains [44]. In this context, we proposed to use NIR spectroscopy and chemometrics to classify each type of grain and flour and attempted to find some variable that is spectrally different.

2. Materials and Methods

2.1. Samples

The samples consisted of five different flours types, in which four were maca, algarrobo, broad bean, soybean, and oatmeal. Maca, algarrobo, and broad bean were purchased from the Hermelinda market in Trujillo, Peru. Moreover, soybean and oatmeal (La Finca, PR, USA) were purchased from Mayaguez Pueblo Supermarket in Puerto Rico. Then, samples were stored in plastic polyethylene bags in a desiccator cabinet. The samples did not undergo any treatment before data acquisition via NIR spectroscopy.

2.2. NIR-FTIR Spectra

The samples were evaluated using Fourier transform near-infrared spectrometer (Bruker Optics; GmbH Ettlingen, Baden-Württemberg, Germany) in the diffuse reflectance mode. The absorption spectra for the samples and the background spectrum were recorded using 32 scans and 32 cm^{-1} resolution. The samples were irradiated using a fiber optic probe, which was connected to the spectrometer, and examined from 4000 to 12,000 cm^{-1}. The fiber optic probe was placed at a height of approximately 1 mm above the sample.

2.3. Spectral Acquisition

A total of 100 g of each flour type was deposited on a small plastic plate. Afterward, 20 different random places were selected in the regions of the small plastic plate that contained the flour. Then, each place was analyzed using NIR spectroscopy. This was performed using PCA and PLS-DA in order to observe whether one type of food was different from the others in terms of spectral shape.

2.4. Spectral Data Analysis

NIR spectral data were analyzed and processed using Unscrambler software, version 10.5 (CAMO, Bedford, MA, USA). Unscrambler software was used to construct the PCA classification models, which were used to analyze the clustering in the data. In addition, the different PCA and PLS-DA models were developed by applying pre-treatments, namely, detrending (2-order), SNV, and Savitzky–Golay first-derivative, and the samples were evaluated individually as well as in a combination of these pretreatments in a spectral region. All PCA and PLS-DA models were analyzed at a 95% confidence level. Meanwhile, Excel 2016 software was used to perform statistical measurements such as determining averages.

3. Results and Discussion

3.1. Spectra Data of Samples That Were Not Pre-Treated

Figure 1 shows the NIR spectra of the soybean, algarrobo, broad bean, maca, and oatmeal samples without pretreatment. Additionally, each sample was assigned a letter and a number: H1—soybean, H2—algarrobo, H3—broad bean, H4—maca, and H5—oatmeal. The raw data spectra showed a change in the baseline values, and it was observed that a set of them presented more intense bands probably caused by the grinding conditions.
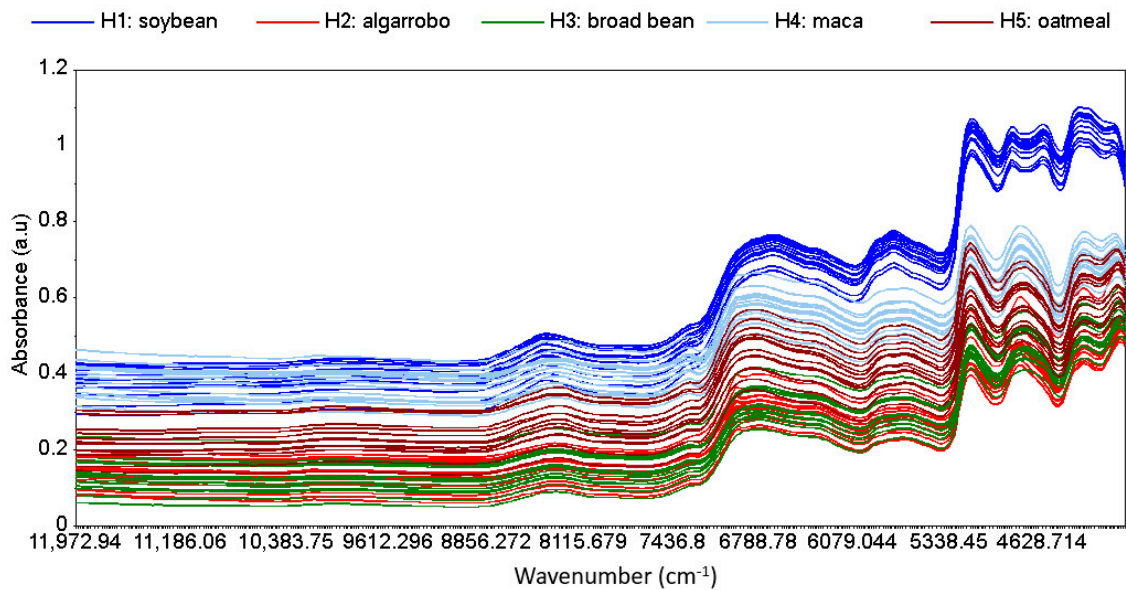
Figure 1. Raw NIR spectra of samples: soybean grain (H1), algarrobo (H2), broad bean (H3), maca (H4), and oatmeal (H5).

For a better visualization of the behavior, the averages of the spectra established for each flour product were obtained. In this case, the soybeans were not in a fine powder form; this could justify their position in the upper zone of the spectra (see Figure 2). However, similar effects of a spectrum baseline shift could be reduced by performing detrending pre-treatment on the data to better visualize the chemical changes between samples. In Figure 2, the characteristic vibrational modes of soybean (H1 mean) can be identified, among which it is important to mention the region from 6000 to 5600 cm^{-1} associated with the C-H functional group, while the N-H and C-O functional groups associated with the proteins lie in the region of 5000–4500 cm^{-1} [45].
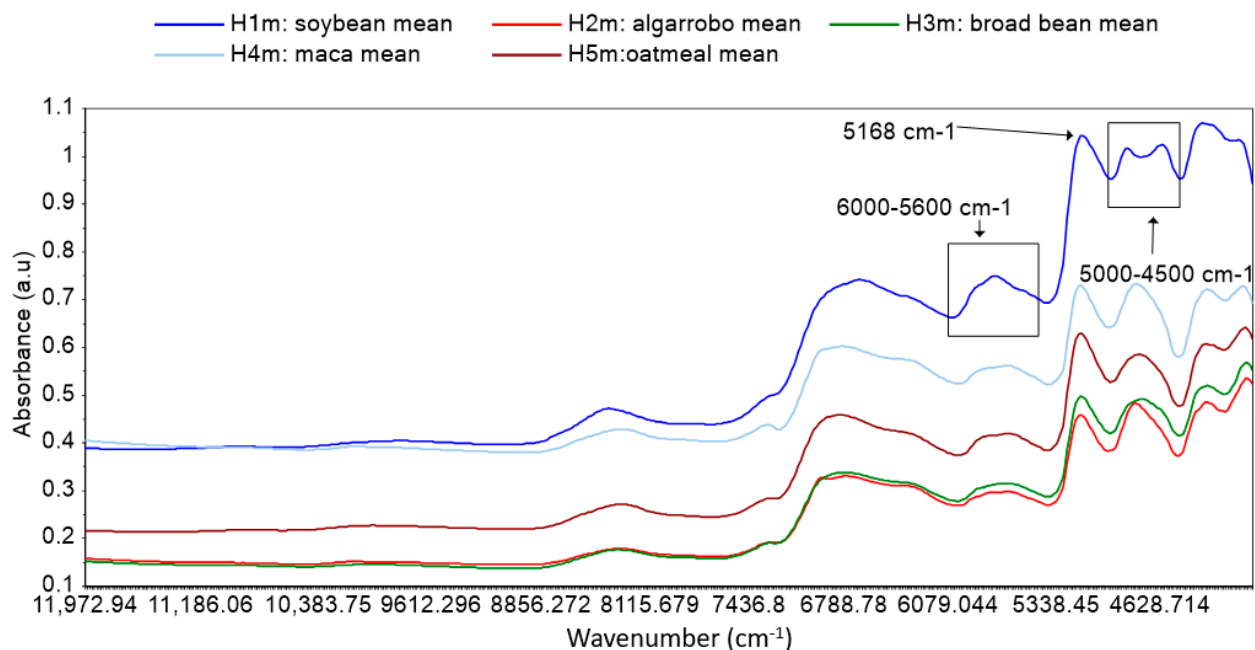
Figure 2. Mean raw spectra obtained from soybean mean (H1m), algarrobo mean (H2m), broad bean mean (H3m), maca mean (H4m), and oatmeal mean (H5m).

3.2. Spectral Data of Pre-Treated Samples

As can be observed in Figure 2, there exists a clear effect of the scattering baseline due to the grain size of soybean and oatmeal [46]. Accordingly, it was helpful to carry out a pre-treatment of the raw data to reduce this effect. Some alternatives are recommended, such as standard normal variation (SNV) and SNV + detrending (two orders) [24,47]. In Figure 3a, we can see that the vertical displacements of the baseline of the spectrum were almost completely corrected, and the differences between the mean spectra of each sample began to be more noticeable after the SNV pre-treatment was employed. The SNV pre-treatment managed to reduce the changes in the baseline, but we can still observe an increasing trend in the slopes of the spectrum bands; this behavior could affect the classification of the sample groups into their main components in the PCA analysis. Therefore, to reduce the changes in the slopes of the spectra in Figure 3a, we applied an SNV + detrending (two-order) pre-treatment. Furthermore, in Figure 3b, the effect of the baseline is visualized; this could be corrected using the first derivative of Savitzky–Golay. This pre-treatment sequence was performed on the raw data, as shown in Figure 3a–c. Differences in absorption spectrum intensities between the samples are best depicted in Figure 3c.
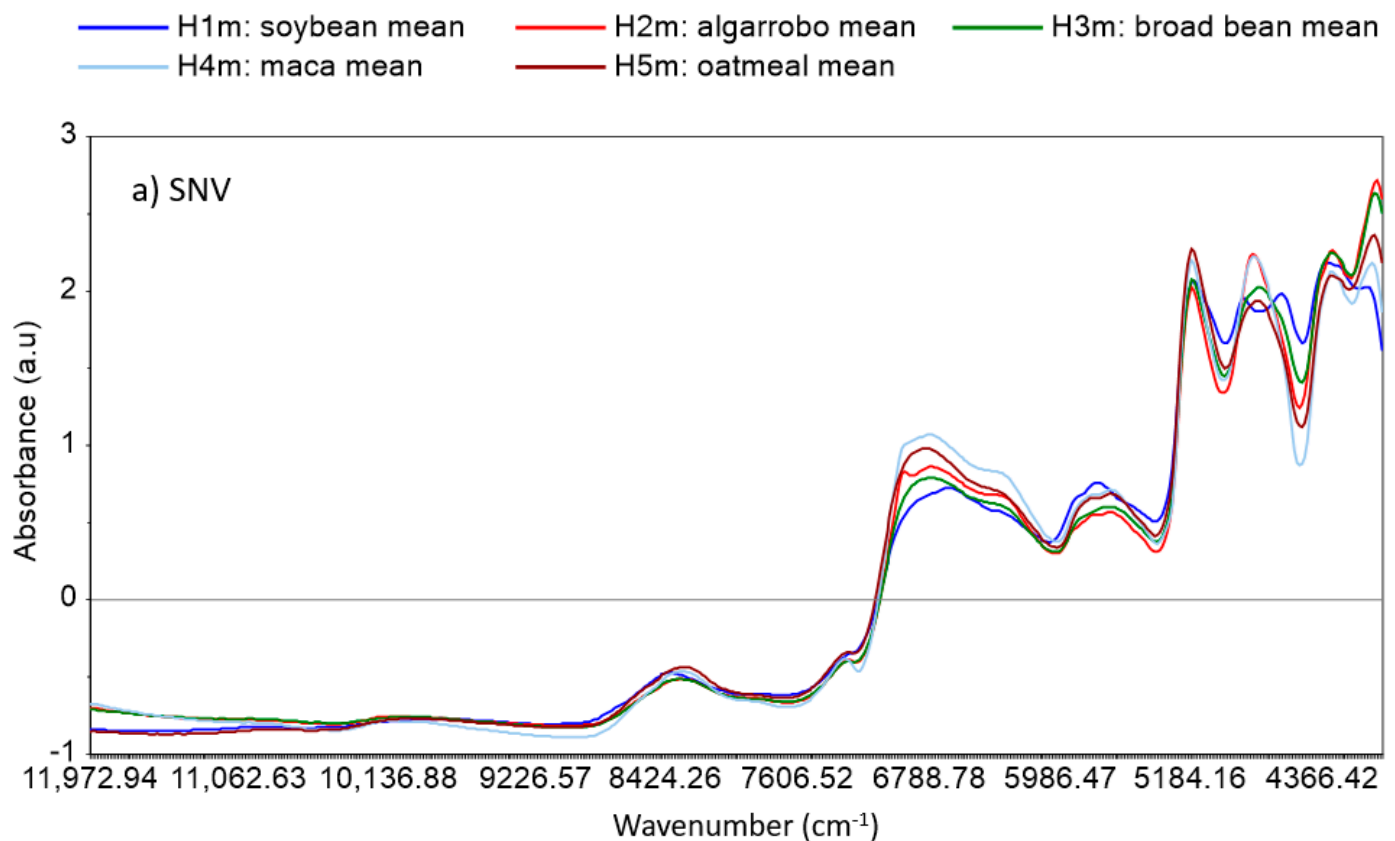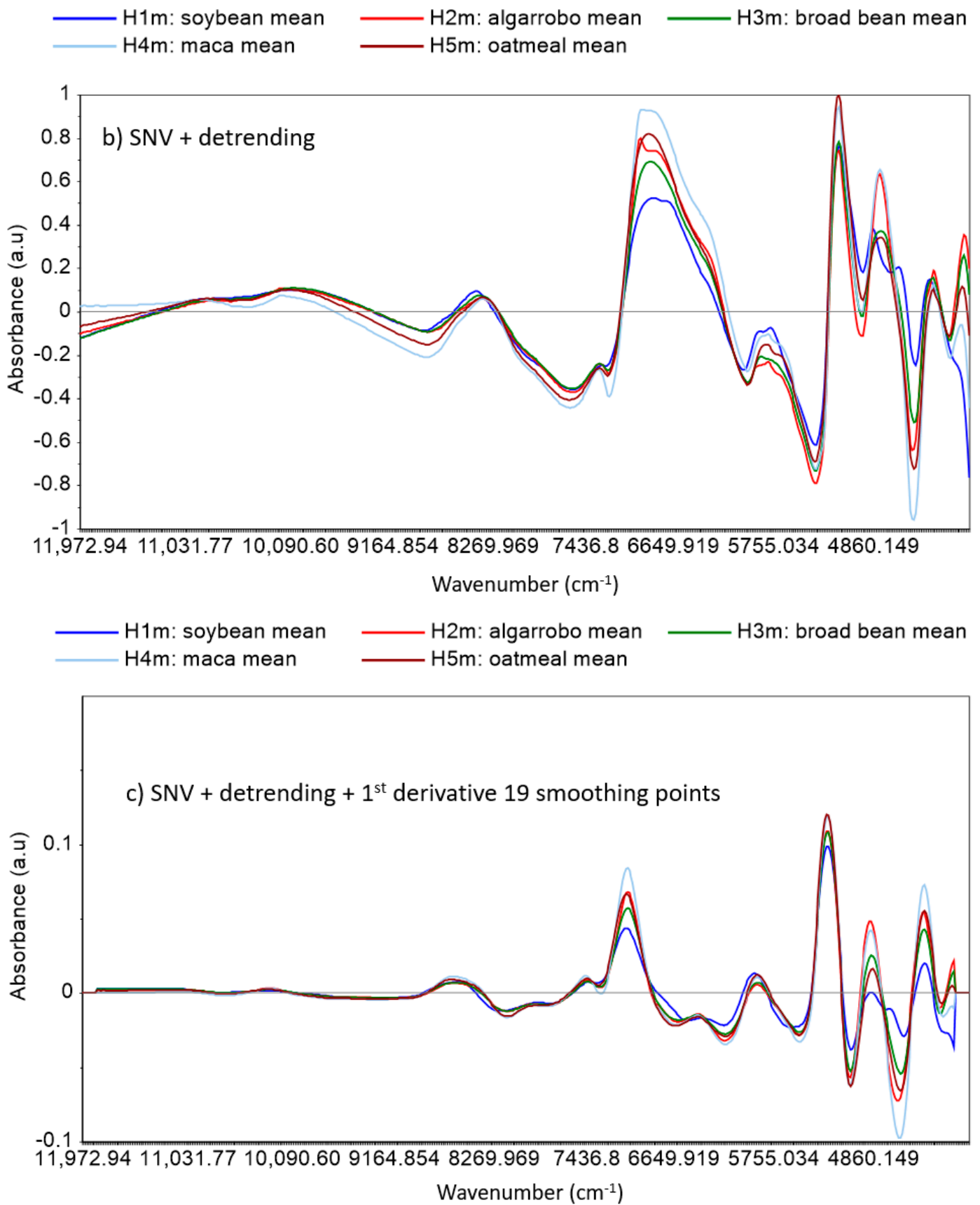

Figure 3. *Cont.*

Figure 3. Pretreatment of spectra for each sample. (**a**) SNV, (**b**) SNV + detrending (2-order), and (**c**) SNV + detrending (2-order) + Savitzky–Golay first-derivative with 19 smoothing points.

3.3. PCA Analysis

PCA is an unsupervised method that reduces variable dimensions into smaller principal components without losing important data. This method is useful because it identifies sources of variance, clustering patterns, trends, and outliers [48,49]. Accordingly, PCA was performed on the raw and pre-treatment data. This was carried out to reveal the effect of pre-treatment and to identify a product from the point of view of the absorbance spectrum.

Figure 4a depicts a spread of data that does not allow for a clear visual separation of the groups, although only two principal components explain the variance of all the data. Moreover, the distance between the groups increased using the SNV pre-treatment, but the number of PCs increased to account for all the explained variance, as shown in Figure 4b and Table 1. Then, the initial pre-treatment led to a good separation between the groups with an increase in the PC [50]. Figure 4c reveals a clear separation of the groups as well as a slight increase in the variation explained by principal component 1 (PC-1) with SNV + pre-treatment with detrending.

Table 1. The behavior of cumulative explained variance as a function of pre-treatment type.

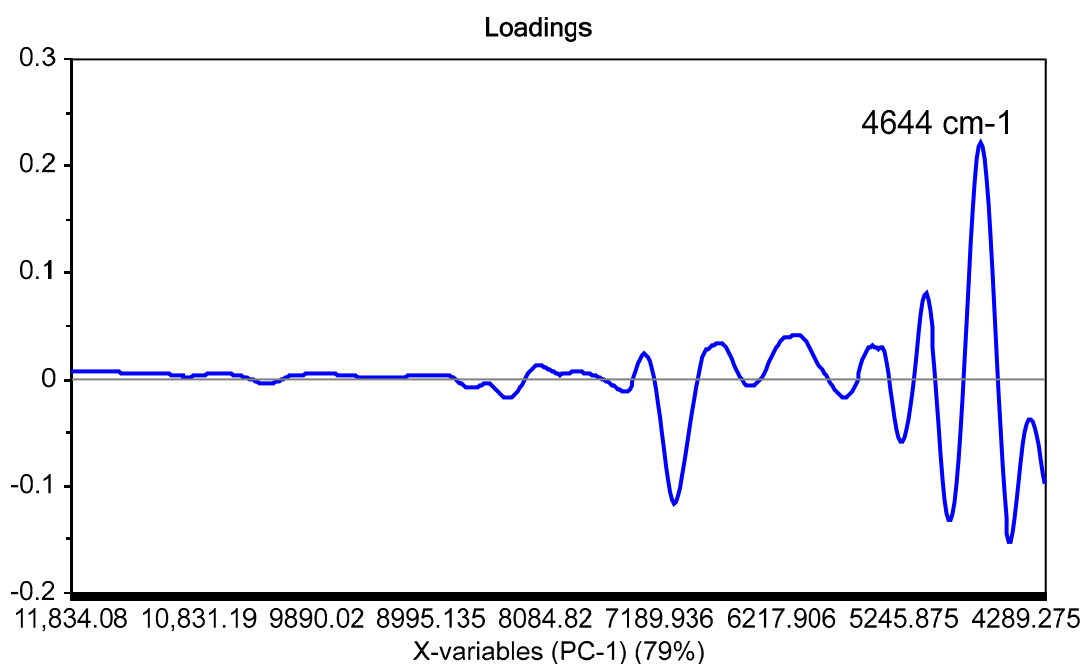| Data Pre-Treatment	Cumulative Explained Variance %				
	PC-1	PC-2	PC-3	PC-4	PC-5
Raw data	95.07	99.85	99.96	99.98	99.99
SNV	50.81	87.85	96.66	98.31	99.47
SNV + detrending	58.77	90.52	97.43	98.93	99.63
SNV + detrending + 1st derivative 19 smoothing points	78.51	91.07	98.10	99.08	99.76
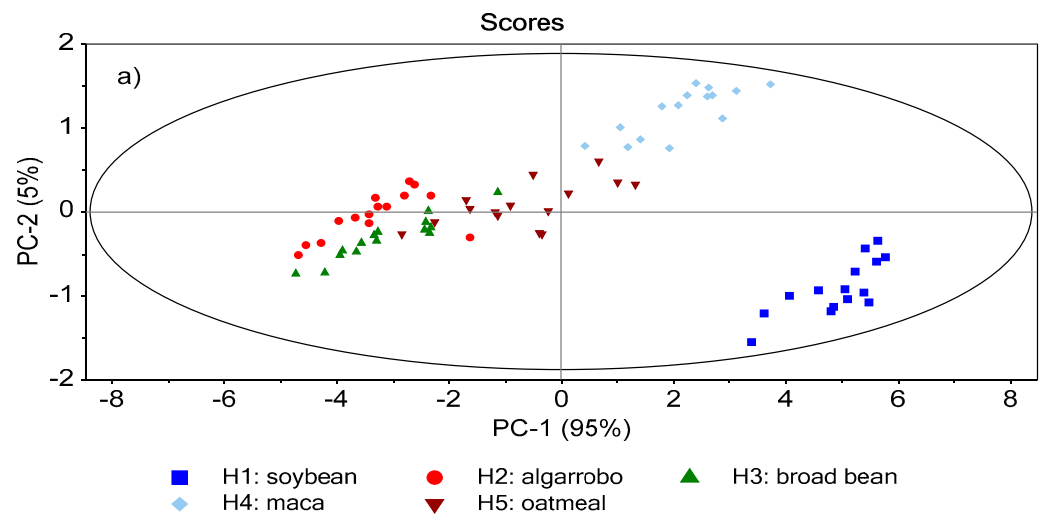
Figure 4. *Cont.*
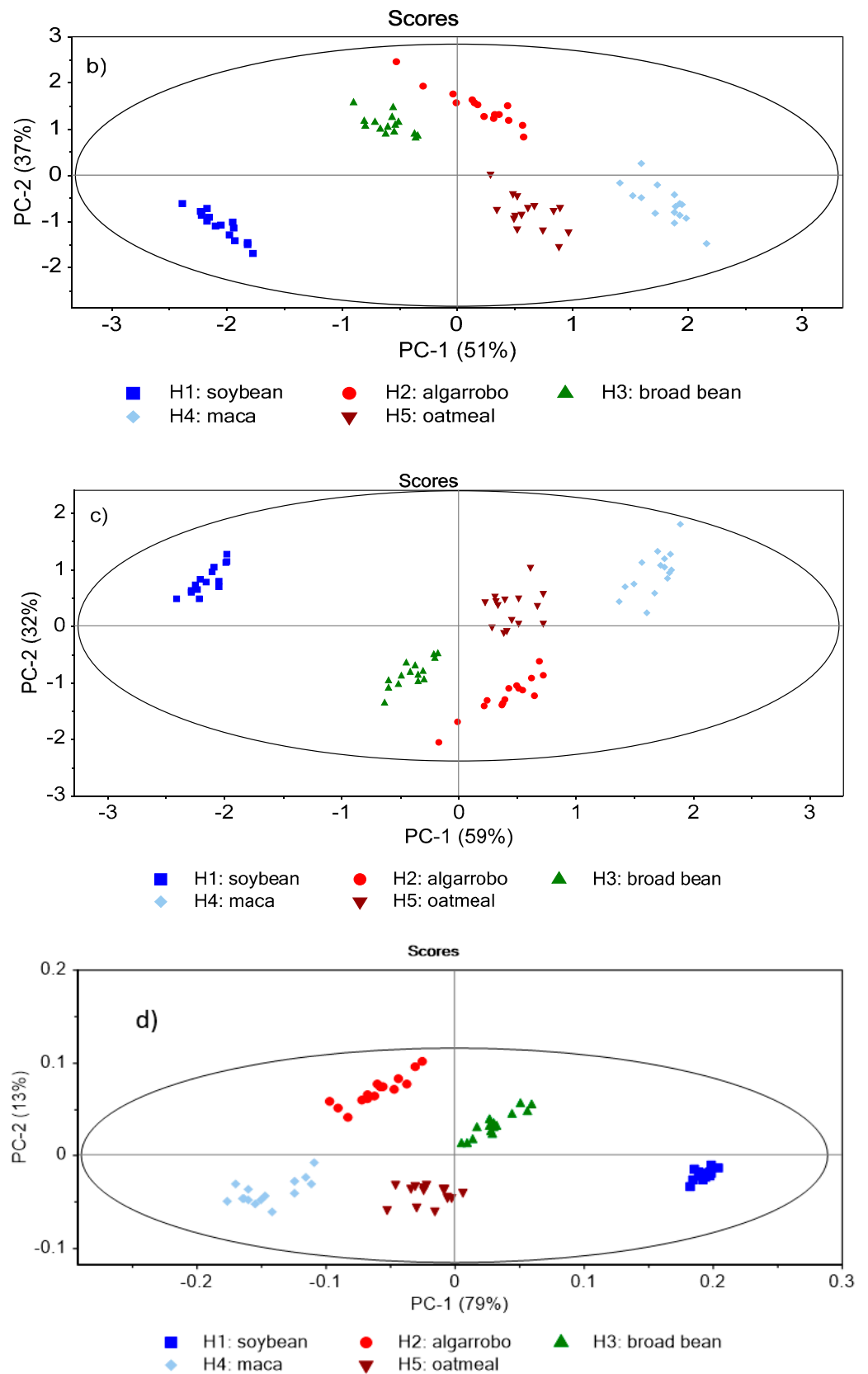
Figure 4. Pretreatment of spectra for each sample. (**a**) Raw data, (**b**) SNV, (**c**) SNV + detrending (2-order), and (**d**) SNV + detrending (2-order) + Savitzky–Golay first-derivative with 19 smoothing points.

The best pre-treatment method for explaining the variances and differences among the flour products was SNV + detrending + 1st derivative with 19 smoothing points, as indicated in Figure 4d. This figure shows the score plot of the five samples, in which soybean is situated on the right side of the central axis, while the other products are near the central axis and the left side. Meanwhile, PC-1 depicts changes at 4644 cm^{-1} due to the increase in C-O bonds in the soybean spectrum, and this result is associated with protein content (see Figure 5) [51,52]. To emphasize, variables with strong positive or negative loading plot values are more representative of the associated principal component; conversely, principal components that have little influence are those that have a loading plot value around 0 [53]. This would indicate that the main source of variation for PC-1 in Figure 4d is the C-O vibrational mode. Importantly, Figure 4d shows a difference between the elements of each cluster for H2–H5 as well as a slight variation for individual samples of H1. This could suggest some heterogeneity within the same cluster for H2–H5. From what has been discussed above, it can be concluded that soybeans are different from the rest. The advantage of creating a PCA classification model with different groups of samples separated with few PCs in a score plot is that one can explain the differences between samples through the variables of the different modes of vibration (wavenumber).


Figure 5. Loading plot for PC-1 to PCA model with SNV + detrending (2-order) + Savitzky–Golay first-derivative with 19 smoothing points.

In reference to the data obtained in Table 1, we can see that the cumulative explained variance changes according to the pre-treatment applied. For example, in the original data, the first three PCs explain almost 100% of the variation present in the samples, but in the score plot of Figure 4a, there is an overlap in the samples that is difficult to explain by means of any difference between them. Figure 3c shows a noticeable difference in the intensities of the vibrational modes of the samples around 4304–8763 cm^{-1}, and this could explain why PC-1 obtains 78% of the variance present in the data without the presence of any sample overlap (Figure 4d).

The first four components for the pre-treatment SNV + detrending + 1st derivative with 19 smoothing points explain almost 100% of the variance present in the samples. Likewise, PC-2, PC-3, and PC-4 contribute 12%, 8%, and 1%, respectively, of the variance explained in the data. But according to Figure 6a,b, these last PCs generate overlaps between a certain group of samples for the remaining score plots, which makes it difficult to observe the

differences between the samples and identify the associated variable. Accordingly, the PCA model of pre-treatment SNV + detrending (2-order) + Savitzky–Golay first-derivative with 19 smoothing points using PC-1 and PC-2 contained sufficient information to explain the separation between the samples.
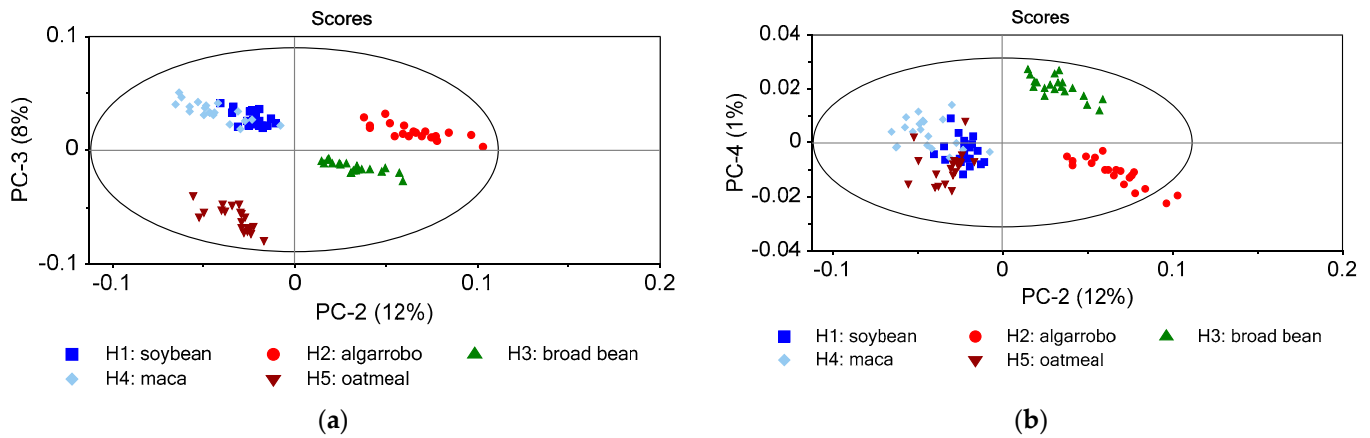
Figure 6. Score plots of PCA model for pre-treatment with SNV + detrending + 1st derivative with 19 smoothing points: (**a**) PC-2 vs. PC-3 score plots, and (**b**) PC-2 vs. PC-4 score plots.

On the other hand, Table 2 describes WI of the samples according to the data obtained by Stevens et al. in the analysis of physical properties using the Whiteness Index between the samples of the H1–H4 group using the values of Hunter scale data, the H1, H3, and H4 samples present very close WI values, visually indicating that the colors of their surfaces are very similar. This is of crucial importance for quality control in the process of mixing powdered flour products [54].

Table 2. Values of Hunter scale and WI for algarrobo, broad bean, maca, and soybean. Data taken and adapted from reference [55].

| Item | Sample | Color | | | |
		L	a	b	WI
1	Algarrobo (H2)	68.92 (0.38)	7.98 (0.17)	33.87 (0.46)	53.34
2	Broad bean (H3)	82.26 (0.43)	1.15 (0.09)	20.06 (0.30)	73.20
3	Yellow maca (H4)	87.35 (0.31)	1.93 (0.04)	23.18 (0.23)	73.52
4	Soybean (H1)	86.99 (0.08)	1.41 (0.08)	23.56 (2.30)	73.05

3.4. PLS-DA Analysis

However, PLS-DA was also applied to classify the flours, as shown in Figure 7a. Figure 7a–c indicate that some samples overlap with other samples of different types, and this behavior made it more difficult to identify which variables allow for differentiation among the samples. Figure 7d shows the score plot for Factor 1 and Factor 2, explaining 85% of the total variance, and it suggests that soybean flour is different from the other samples; this is explained in Figure 2, in which the soybean sample displays two bands in the 4500–5000 cm^{-1} region. Meanwhile, the other samples show one band in this region. Oatmeal flour displays a remarkable internal variation between them; meanwhile, broad bean flour shows a slight internal variation. Broad bean and algarrobo flour are similar due to the fact that the broad bean and algarrobo clusters are closer; this situation is evidenced in Figure 2. Additionally, the value of the loading plot for LV1 in each PLS-DA model is low (as indicates Figure 8), which suggests that the variables are not relevant enough to explain the associated LV.
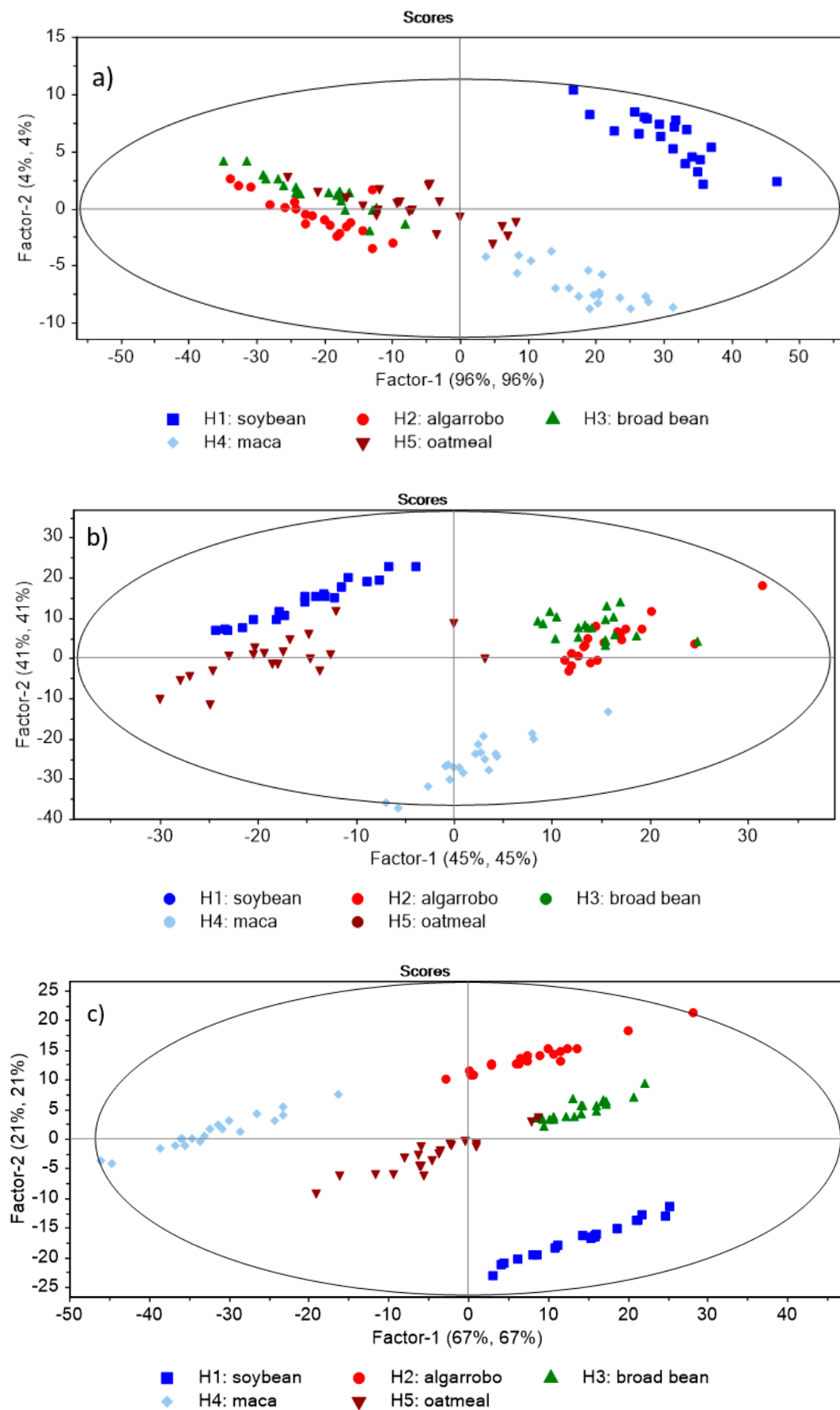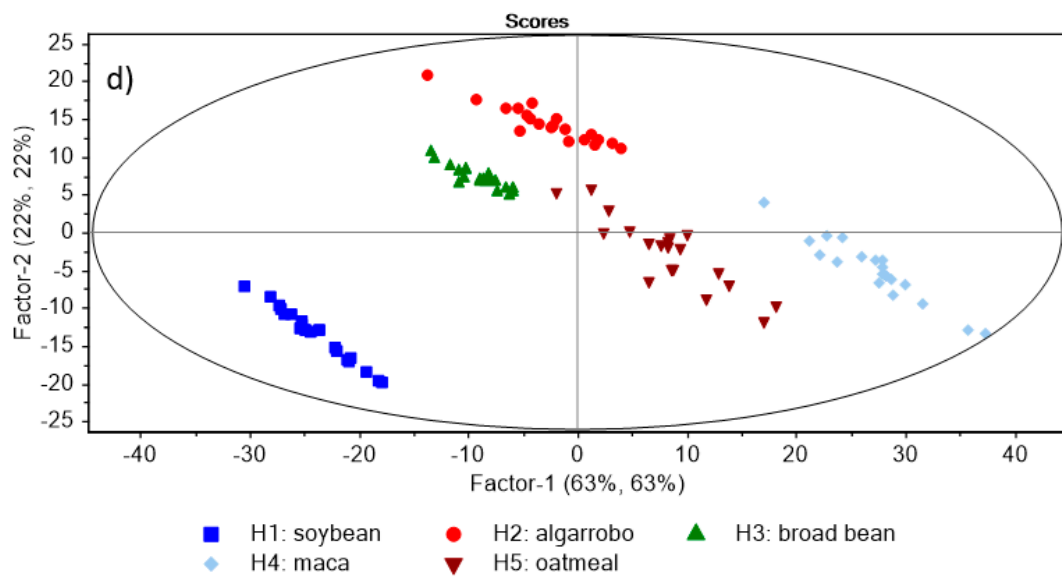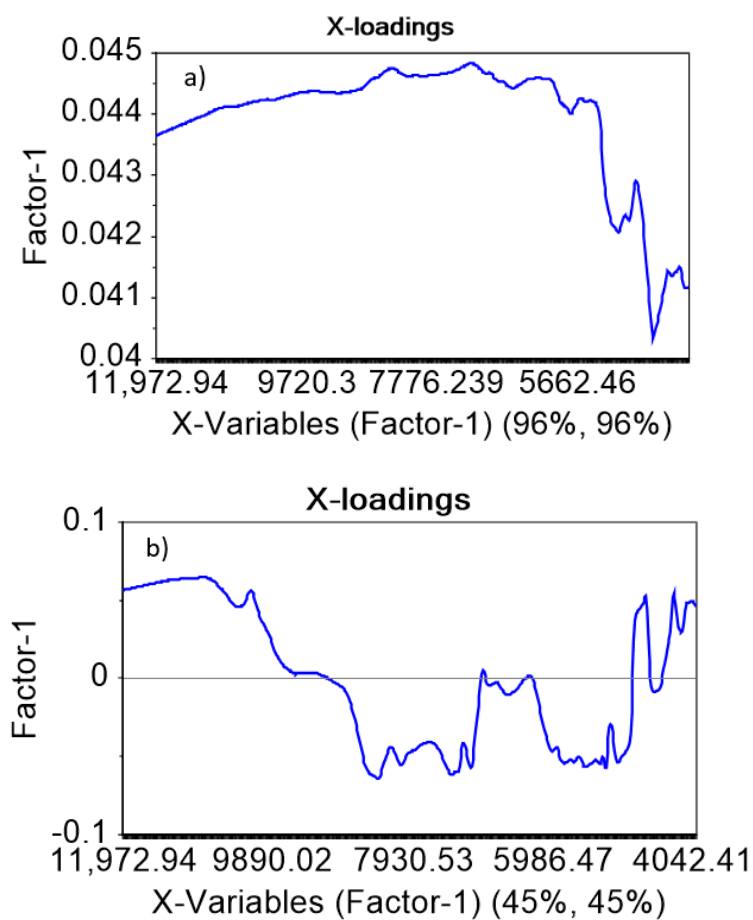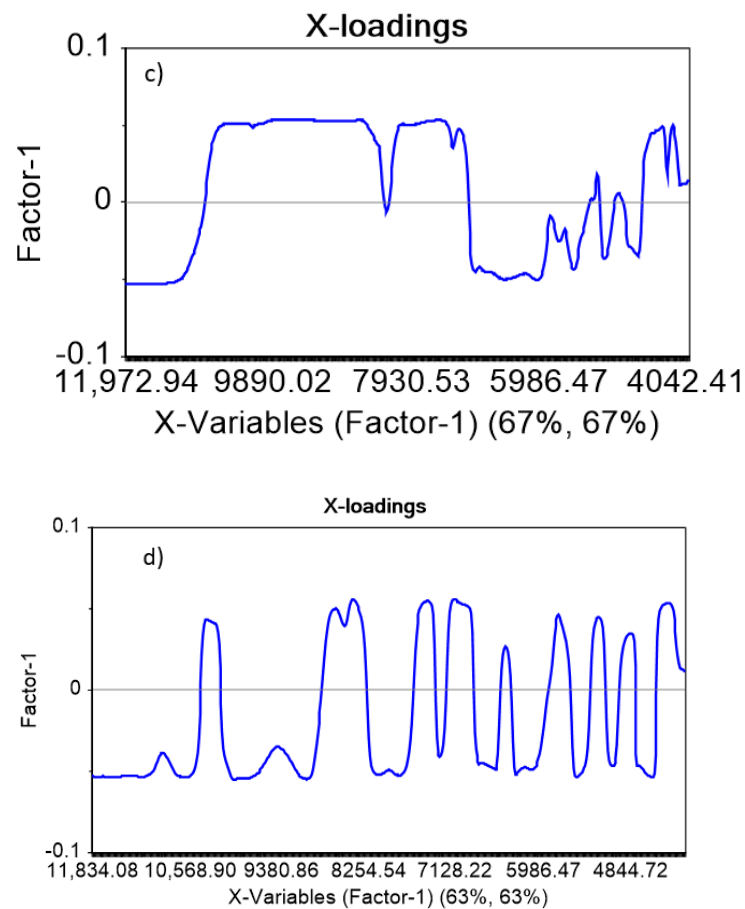
Figure 7. *Cont.*

Figure 7. PLS-DA score plot (LV1 vs. LV2) in the analysis of the spectra (12,000–4000 cm^{-1} range) for (**a**) raw data, (**b**) SNV, (**c**) SNV + detrending (2-order), and (**d**) SNV + detrending (2-order) + Stavisky–Golay first-derivative with 19 smoothing points. LV: Latent Variable.

Figure 8. *Cont.*

Figure 8. Loading plot for PC-1 for the PLS-DA model with (**a**) raw data, (**b**) SNV, (**c**) SNV + detrending (2-order), and (**d**) SNV + detrending (2-order) + Savitzky–Golay first-derivative with 19 smoothing points. LV: Latent Variable.

The loading plot for Factor 1 in Figure 8c shows 10 relevant variables (wavenumbers) in the 10,400–4397 cm^{-1} region that explain 63% of the data retained by Factor 1, and this indicates that 10 variables could explain the classification and differentiation between samples. Meanwhile, the loading plot for PC-1 in Figure 5 suggests that one relevant variable at 4644 cm^{-1} describes the variation between the samples. As mentioned above, Figure 4c shows better separation of the groups than Figure 7d, and this allowed it to describe the variables that explain the differences between the samples most accurately.

4. Conclusions

In the present work, chemometrics analysis was performed to classify healthy and nutritious flour products using NIR spectroscopy. PCA allowed for the discrimination and identification of more spectral samples, basically via increasing the band to 4644 cm^{-1} associated with the C-H link. Furthermore, the ability to differentiate soybean from maca, algarrobo, broad bean, and oatmeal allowed for their identification in a mixture containing H1–H5 flour. The results suggest a promising route for using NIR spectroscopy and chemometrics to understand the quality of these Peruvians flours, opening new possibilities for their use as tools in the quality control of processed flour products.

Author Contributions: Conceptualization, M.M.-J., R.N.-N. and M.G.-C.; methodology, M.M.-J. and H.C.-E.; software, H.C.-E. and A.A.-E.; validation, M.M.-J. and S.R.-F.; formal analysis, M.M.-J., M.G.-C. and E.M.-T.; investigation, M.M.-J. and R.N.-N.; data curation, S.R.-F., H.C.-E. and A.A.-E.; writing—original draft preparation, M.M.-J. and E.M.-T.; writing—review and editing, R.N.-N. and M.G.-C.; project administration, M.M.-J. All authors have read and agreed to the published version of the manuscript.

References

1. Da Silva Leitão Peres, N.; Cabrera Parra Bortoluzzi, L.; Medeiros Marques, L.L.; Formigoni, M.; Fuchs, R.H.B.; Droval, A.A.; Reitz Cardoso, F.A. Medicinal Effects of Peruvian Maca (*Lepidium meyenii*): A Review. *Food Funct.* **2020**, *11*, 83–92. [CrossRef] [PubMed]
2. Harina de Habas, Kiwicha y Pan Con Queso Incluyó el Desayuno de Qali Warma|Noticias|Agencia Peruana de Noticias Andina. Available online: https://andina.pe/agencia/noticia-harina-habaskiwicha-y-pan-queso-incluyo-desayuno-qali-warma-4972 05.aspx (accessed on 28 May 2022).
3. Xia, C.; Chen, J.; Deng, J.L.; Zhu, Y.Q.; Li, W.Y.; Jie, B.; Chen, T.Y. Novel Macamides from Maca (*Lepidium meyenii* Walpers) Root and Their Cytotoxicity. *Phytochem. Lett.* **2018**, *25*, 65–69. [CrossRef]
4. Felker, P.; Grados, N.; Cruz, G.; Prokopiuk, D. Economic Assessment of Production of Flour from Prosopis Alba and *P. Pallida* Pods for Human Food Applications. *J. Arid Environ.* **2003**, *53*, 517–528. [CrossRef]
5. Yatsu, F.K.J.; Koester, L.S.; Bassani, V.L. Isoflavone-Aglycone Fraction from Glycine Max: A Promising Raw Material for Isoflavone-Based Pharmaceutical or Nutraceutical Products. *Rev. Bras. Farmacogn.* **2016**, *26*, 259–267. [CrossRef]
6. Rasane, P.; Jha, A.; Sabikhi, L.; Kumar, A.; Unnikrishnan, V.S. Nutritional Advantages of Oats and Opportunities for Its Processing as Value Added Foods—A Review. *J. Food Sci. Technol.* **2015**, *52*, 662–675. [CrossRef]
7. Ramírez-Moreno, J.M.; Salguero Bodes, I.; Romaskevych, O.; Duran-Herrera, M.C. Broad Bean (*Vicia faba*) Consumption and Parkinson's Disease: A Natural Source of L-Dopa to Consider. *Neurologia* **2015**, *30*, 375–391. [CrossRef]
8. Gafner, S.; Blumenthal, M.; Foster, S.; John, H.; Cardellina, I.; Khan, I.A.; Upton, R. Botanical Ingredient Forensics: Detection of Attempts to Deceive Commonly Used Analytical Methods for Authenticating Herbal Dietary and Food Ingredients and Supplements. *J. Nat. Prod.* **2023**, *86*, 460–472. [CrossRef]
9. Schmitt, C.; Bastek, T.; Stelzer, A.; Schneider, T.; Fischer, M.; Hackl, T. Detection of Peanut Adulteration in Food Samples by Nuclear Magnetic Resonance Spectroscopy. *J. Agric. Food Chem.* **2020**, *68*, 14364–14373. [CrossRef]
10. Lermen, F.H.; Echeveste, M.E.; Peralta, C.B.; Sonego, M.; Marcon, A. A Framework for Selecting Lean Practices in Sustainable Product Development: The Case Study of a Brazilian Agroindustry. *J. Clean. Prod.* **2018**, *191*, 261–272. [CrossRef]
11. Martins, M.S.; Nascimento, M.H.; Barbosa, L.L.; Campos, L.C.G.; Singh, M.N.; Martin, F.L.; Romão, W.; Filgueiras, P.R.; Barauna, V.G. Detection and Quantification Using ATR-FTIR Spectroscopy of Whey Protein Concentrate Adulteration with Wheat Flour. *LWT* **2022**, *172*, 114161. [CrossRef]
12. Yang, X.; Xing, B.; Guo, Y.; Wang, S.; Guo, H.; Qin, P.; Hou, C.; Ren, G. Rapid, Accurate and Simply-Operated Determination of Laboratory-Made Adulteration of Quinoa Flour with Rice Flour and Wheat Flour by Headspace Gas Chromatography-Ion Mobility Spectrometry. *LWT* **2022**, *167*, 113814. [CrossRef]
13. Curzon, A.Y.; Chandrasekhar, K.; Nashef, Y.K.; Abbo, S.; Bonfil, D.J.; Reifen, R.; Bar-El, S.; Avneri, A.; Ben-David, R. Distinguishing between Bread Wheat and Spelt Grains Using Molecular Markers and Spectroscopy. *J. Agric. Food Chem.* **2019**, *67*, 3837–3841. [CrossRef]
14. da Costa Filho, P.A.; Cobuccio, L.; Mainali, D.; Rault, M.; Cavin, C. Rapid Analysis of Food Raw Materials Adulteration Using Laser Direct Infrared Spectroscopy and Imaging. *Food Control* **2020**, *113*, 107114. [CrossRef]
15. Xue, S.S.; Tan, J.; Xie, J.Y.; Li, M.F. Rapid, Simultaneous and Non-Destructive Determination of Maize Flour and Soybean Flour Adulterated in Quinoa Flour by Front-Face Synchronous Fluorescence Spectroscopy. *Food Control* **2021**, *130*, 108329. [CrossRef]
16. Kokesch-Himmelreich, J.; Wittek, O.; Race, A.M.; Rakete, S.; Schlicht, C.; Busch, U.; Römpp, A. MALDI Mass Spectrometry Imaging: From Constituents in Fresh Food to Ingredients, Contaminants and Additives in Processed Food. *Food Chem.* **2022**, *385*, 132529. [CrossRef]
17. Ghafori, S.; Habibipour, R.; Bayat, S. Optimization of a Real-Time PCR Assay for Identification of Aspergillus Fumigatus and Aspergillus Niger from Flour Samples: Comparison of Phenotypic and Genotypic Methods. *Gene Rep.* **2021**, *22*, 100993. [CrossRef]
18. Narukawa, T.; Chiba, K.; Sinaviwat, S.; Feldmann, J. A Rapid Monitoring Method for Inorganic Arsenic in Rice Flour Using Reversed Phase-High Performance Liquid Chromatography-Inductively Coupled Plasma Mass Spectrometry. *J. Chromatogr. A* **2017**, *1479*, 129–136. [CrossRef]
19. Zhao, L.; Hu, Y.; Liu, W.; Wu, H.; Xiao, J.; Zhang, C.; Zhang, H.; Zhang, X.; Liu, J.; Lu, X.; et al. Identification of Camel Species in Food Products by a Polymerase Chain Reaction-Lateral Flow Immunoassay. *Food Chem.* **2020**, *319*, 126538. [CrossRef]

20. Rolandelli, G.; Farroni, A.E.; del Pilar Buera, M. Analysis of Molecular Mobility in Corn and Quinoa Flours through 1H NMR and Its Relationship with Water Distribution, Glass Transition and Enthalpy Relaxation. *Food Chem.* **2022**, *373*, 131422. [CrossRef]
21. Nivelle, M.A.; Remmerie, E.; Bosmans, G.M.; Vrinten, P.; Nakamura, T.; Delcour, J.A. Amylose and Amylopectin Functionality during Baking and Cooling of Bread Prepared from Flour of Wheat Containing Unusual Starches: A Temperature-Controlled Time Domain 1H NMR Study. *Food Chem.* **2019**, *295*, 110–119. [CrossRef]
22. Tian, Y.; He, Q.; Chen, X.; Wang, S. Nuclear Magnetic Resonance Spectroscopy for Food Quality Evaluation. *Eval. Technol. Food Qual.* **2019**, 193–217. [CrossRef]
23. Czaja, T.; Mazurek, S.; Szostak, R. Quantification of Gluten in Wheat Flour by FT-Raman Spectroscopy. *Food Chem.* **2016**, *211*, 560–563. [CrossRef]
24. Adedipe, O.E.; Johanningsmeier, S.D.; Den Truong, V.; Yencho, G.C. Development and Validation of a Near-Infrared Spectroscopy Method for the Prediction of Acrylamide Content in French-Fried Potato. *J. Agric. Food Chem.* **2016**, *64*, 1850–1860. [CrossRef]
25. Liu, Y.; He, Z.; Shankle, M.; Tewolde, H. Compositional Features of Cotton Plant Biomass Fractions Characterized by Attenuated Total Reflection Fourier Transform Infrared Spectroscopy. *Ind. Crops Prod.* **2016**, *79*, 283–286. [CrossRef]
26. Lazzari, E.; Schena, T.; Marcelo, M.C.A.; Primaz, C.T.; Silva, A.N.; Ferrão, M.F.; Bjerk, T.; Caramão, E.B. Classification of Biomass through Their Pyrolytic Bio-Oil Composition Using FTIR and PCA Analysis. *Ind. Crops Prod.* **2018**, *111*, 856–864. [CrossRef]
27. Esbensen, K.; Guyot, D.; Westad, F.; Houmoller, L.P. *Multivariate Data Analysis: In Practice: An Introduction to Multivariate Data Analysis and Experimental Design*; CAMO: Pinehurst, TX, USA, 1994.
28. Beiras, R. Pollution Control. In *Marine Pollution*; Elsevier: Amsterdam, The Netherlands, 2018; pp. 329–354. [CrossRef]
29. Granato, D.; Santos, J.S.; Escher, G.B.; Ferreira, B.L.; Maggio, R.M. Use of Principal Component Analysis (PCA) and Hierarchical Cluster Analysis (HCA) for Multivariate Association between Bioactive Compounds and Functional Properties in Foods: A Critical Perspective. *Trends Food Sci. Technol.* **2018**, *72*, 83–90. [CrossRef]
30. Lee, L.C.; Liong, C.Y.; Jemain, A.A. Partial least squares-discriminant analysis (PLS-DA) for classification of high-dimensional (HD) data: A review of contemporary practice strategies and knowledge gaps. *Analyst* **2018**, *143*, 3526–3539. [CrossRef]
31. Bylesjö, M.; Rantalainen, M.; Cloarec, O.; Nicholson, J.K.; Holmes, E.; Trygg, J. OPLS discriminant analysis: Combining the strengths of PLS-DA and SIMCA classification. *J. Chemom. A J. Chemom. Soc.* **2006**, *20*, 341–351. [CrossRef]
32. Ballabio, D.; Consonni, V. Classification tools in chemistry. Part 1: Linear models. PLS-DA. *Anal. Methods* **2013**, *5*, 3790–3798. [CrossRef]
33. Lasalvia, M.; Capozzi, V.; Perna, G. A comparison of PCA-LDA and PLS-DA techniques for classification of vibrational spectra. *Appl. Sci.* **2022**, *12*, 5345. [CrossRef]
34. Sierra-Vega, N.O.; Sánchez-Paternina, A.; Maldonado, N.; Cárdenas, V.; Romañach, R.J.; Méndez, R. In Line Monitoring of the Powder Flow Behavior and Drug Content in a Fette 3090 Feed Frame at Different Operating Conditions Using Near Infrared Spectroscopy. *J. Pharm. Biomed. Anal.* **2018**, *154*, 384–396. [CrossRef]
35. Sun, D.-W. *Infrared Spectroscopy for Food Quality Analysis and Control*; Academic Press: Cambridge, MA, USA; Elsevier: Amsterdam, The Netherlands, 2009.
36. Lee, L.C.; Liong, C.-Y.; Jemain, A.A. A Contemporary Review on Data Preprocessing (DP) Practice Strategy in ATR-FTIR Spectrum. *Chemom. Intell. Lab. Syst.* **2017**, *163*, 64–75. [CrossRef]
37. Lasch, P. Spectral Pre-Processing for Biomedical Vibrational Spectroscopy and Microspectroscopic Imaging. *Chemom. Intell. Lab. Syst.* **2012**, *117*, 100–114. [CrossRef]
38. Li, P.; Zhang, X.; Li, S.; Du, G.; Jiang, L.; Liu, X.; Ding, S.; Shan, Y. A Rapid and Nondestructive Approach for the Classification of Different-Age Citri Reticulatae Pericarpium Using Portable Near Infrared Spectroscopy. *Sensors* **2020**, *20*, 1586. [CrossRef]
39. González-Fernández, A.B.; Sanz-Ablanedo, E.; Gabella, V.M.; García-Fernández, M.; Rodríguez-Pérez, J.R. Field Spectroscopy: A Non-Destructive Technique for Estimating Water Status in Vineyards. *Agronomy* **2019**, *9*, 427. [CrossRef]
40. Shotts, M.L.; Plans Pujolras, M.; Rossell, C.; Rodriguez-Saona, L. Authentication of Indigenous Flours (Quinoa, Amaranth and Kañiwa) from the Andean Region Using a Portable ATR-Infrared Device in Combination with Pattern Recognition Analysis. *J. Cereal Sci.* **2018**, *82*, 65–72. [CrossRef]
41. Kniese, J.; Race, A.M.; Schmidt, H. Classification of Cereal Flour Species Using Raman Spectroscopy in Combination with Spectra Quality Control and Multivariate Statistical Analysis. *J. Cereal Sci.* **2021**, *101*, 103299. [CrossRef]
42. Ding, X.; Ni, Y.; Kokot, S. NIR Spectroscopy and Chemometrics for the Discrimination of Pure, Powdered, Purple Sweet Potatoes and Their Samples Adulterated with the White Sweet Potato Flour. *Chemom. Intell. Lab. Syst.* **2015**, *144*, 17–23. [CrossRef]
43. Ayvaz, H.; Korkmaz, F.; Polat, H.; Ayvaz, Z.; Barış Tuncel, N. Detection of Einkorn Flour Adulteration in Flour and Bread Samples Using Computer-Based Image Analysis and Near-Infrared Spectroscopy. *Food Control* **2021**, *127*, 108162. [CrossRef]
44. Verdú, S.; Ivorra, E.; Sánchez, A.J.; Barat, J.M.; Grau, R. Study of High Strength Wheat Flours Considering Their Physicochemical and Rheological Characterisation as Well as Fermentation Capacity Using SW-NIR Imaging. *J. Cereal Sci.* **2015**, *62*, 31–37. [CrossRef]
45. Amanah, H.Z.; Joshi, R.; Masithoh, R.E.; Choung, M.G.; Kim, K.H.; Kim, G.; Cho, B.K. Nondestructive Measurement of Anthocyanin in Intact Soybean Seed Using Fourier Transform Near-Infrared (FT-NIR) and Fourier Transform Infrared (FT-IR) Spectroscopy. *Infrared Phys. Technol.* **2020**, *111*, 103477. [CrossRef]
46. Bazoni, C.H.V.; Ida, E.I.; Barbin, D.F.; Kurozawa, L.E. Near-Infrared Spectroscopy as a Rapid Method for Evaluation Physico-chemical Changes of Stored Soybeans. *J. Stored Prod. Res.* **2017**, *73*, 1–6. [CrossRef]

47. Zhu, Z.; Chen, S.; Wu, X.; Xing, C.; Yuan, J. Determination of Soybean Routine Quality Parameters Using Near-infrared Spectroscopy. *Food Sci. Nutr.* **2018**, *6*, 1109. [CrossRef] [PubMed]
48. Garip, S.; Bayari, S.H.; Severcan, M.; Abbas, S.; Lednev, I.K.; Severcan, F. Structural Effects of Simvastatin on Rat Liver Tissue: Fourier Transform Infrared and Raman Microspectroscopic Studies. *J. Biomed. Opt.* **2016**, *21*, 025008. [CrossRef]
49. Adnan, A.; von Hörsten, D.; Pawelzik, E.; Mörlein, D. Rapid Prediction of Moisture Content in Intact Green Coffee Beans Using Near Infrared Spectroscopy. *Foods* **2017**, *6*, 38. [CrossRef]
50. Tamburini, E.; Uria, C.F.L.; Dedenaro, G.; Costa, S.; Marchetti, M.G.; Pedrini, P. Potential of Near Infrared Spectroscopy for Classification of Different Delignificant Pre-Treatments on Banana Rachis. *J. Anal. Bioanal. Tech.* **2016**, *7*, 311. [CrossRef]
51. Shenk, J.S.; Workman, J.J.; Westerhaus, M.O. Application of NIR Spectroscopy to Agricultural Products. In *Handbook of Near-Infrared Analysis*, 3rd ed.; CRC Press: Boca Raton, FL, USA, 2007; pp. 347–386. [CrossRef]
52. Ferreira, D.S.; Galão, O.F.; Pallone, J.A.L.; Poppi, R.J. Comparison and Application of Near-Infrared (NIR) and Mid-Infrared (MIR) Spectroscopy for Determination of Quality Parameters in Soybean Samples. *Food Control* **2014**, *35*, 227–232. [CrossRef]
53. He, S.; Xie, W.; Zhang, W.; Zhang, L.; Wang, Y.; Liu, X.; Liu, Y.; Du, C. Multivariate Qualitative Analysis of Banned Additives in Food Safety Using Surface Enhanced Raman Scattering Spectroscopy. *Spectrochim. Acta Part A Mol. Biomol. Spectrosc.* **2015**, *137*, 1092–1099. [CrossRef]
54. Canovas, G.V.B.; Juliano, P. *Food Powders: Physical Properties, Processing and Functionality*; Springer: Berlin/Heidelberg, Germany, 2005.
55. Raúl, R. *Near-Infrared Spectroscopy with Chemometrics for the Rapid Authentication and Quantification of Crop Flours*; Universidad del Atlántico: Barranquilla, Colombia, 2020.